

Analysis of an Aterally Loaded Pile under Scour Conditions Using Particle Image Velocimetry (PIV) Technique

Xiaofeng YANG, Zhenwei HE, Feng YU*

Abstract: Scouring, which is a common occurrence around pile foundations of bridges and offshore structures, poses a significant threat to their safety. Presently, research on scour has primarily focused on assessing the maximum scour depth, understanding the scour mechanism, and studying the degradation of the bearing capacity of pile foundations caused by scouring effects. However, there is limited research on the deformation characteristics of the soil around a laterally loaded pile with a three-dimensional (3D) scour hole. In this study, a series of model tests on laterally loaded piles were conducted in sand using the particle image velocimetry (PIV) technique. The effects of sand relative density, stiffness of the pile shaft, and size of the 3D scour hole were considered. The experimental results indicate that as the lateral load increases, the soil strain in the passive zone around the pile gradually develops in both radial and vertical directions, irrespective of the presence of scour. Additionally, due to pile movement, the soil in the active zone behind the pile may slide into a gap behind the pile shaft.

Keywords: lateral load; pile; PIV; sand; scour; soil strain field

1 INTRODUCTION

Pile foundations have been extensively used in projects involving ports, bridges, and offshore wind energy generation. In deep water situations, pile foundations must be able to bear not only the vertical loads transferred by the above structure, but also the lateral loads brought on by strong winds, floods, waves, and impacts. Additionally, flowing water will also erode the soil around the pile foundation and gradually form a three-dimensional (3D) scour hole. The loss of local soil layers around the pile will ultimately increase the pile shaft's bending moment at the post-ground surface and decrease the effective self-weight stress of the remaining soil layer, which may decrease the horizontal bearing capacity of the pile foundation. Therefore, the research on the horizontal bearing characteristics of pile foundations under scour conditions is increasingly being paid attention to by geotechnical engineering scholars and technicians.

Numerous studies on scour concentrate on the mechanism of soil erosion, estimation of the maximum scour depth, scour protection [1-4], while there are limited studies on scouring effects on behaviour of laterally loaded pile foundations [5-7]. Two different types of scour are typically recognised when investigating the effects of scouring on the lateral bearing capacity of pile foundations [8]: general scour (erosion across the entire superficial soil layer) and local scour (erosion generating a 3D conical scour hole around the pile foundation). As shown in Fig. 1, a local scour hole around the pile foundation can be represented by three factors: scour depth (S_d), scour width (S_w), and scour slope (θ), and the general scour can be regarded as a special case of local scour with a slope angle of 0° . Both general scour and local scour result in a reduction in pile embedment and an increase in the load eccentricity from e to e' , causing much larger lateral deformations of the pile shaft. According to centrifuge model studies in [8], the difference between general and local scour can be attributed to the latter's advantageous influence of the remaining overburden soil around the pile. Ignoring the whole soil layer above the post-scour ground line is conservative for analyzing the scour effects on the lateral pile response. Although these theoretical and

experimental studies have improved the understanding of the scouring effect on laterally loaded pile foundations, the deformation characteristics of pile-soil systems subjected to lateral loads at the pile head are not readily apparent.

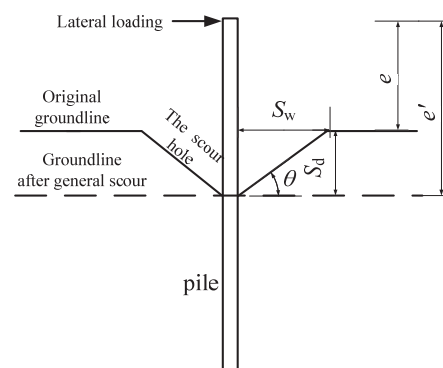


Figure 1 Local scour or general scour around a laterally loaded pile

Particle image velocimetry (PIV) or digital image correlation (DIC) technique, which has been successfully applied in soil mechanics and geotechnical problems [9-11], offers an important way to analyse soil-structure interaction from a visual perspective. The PIV or DIC technique has also been used for piling foundations. Hajjalilue-Bonab et al. (2013) carried out a series of lateral loading tests on a small-scale single pile in loose sand [12]. They used PIV analysis to extract the soil displacement vectors and strain fields, and recommended a 3D strain wedge in the form of a cone. Suleiman et al. (2015) used DIC data to demonstrate soil movement up to 6.3 pile diameters from the pile center in a model test of a 1.42 m long, 102 mm diameter precast concrete pile subjected to lateral loading [13]. Yuan et al. (2019) developed a 3D displacement monitoring system on the basis of transparent soil tests and PIV technique for lateral soil-pile interaction [14]. All of those studies have aided in our understanding of the lateral soil-pile interaction, but they neglected to consider the impact that scour would have on the lateral response of pile foundations.

In order to obtain the soil displacement fields and strain fields surrounding the pile and analyze the distribution and evolution properties of soil strain, a series

of model tests of laterally loaded piles using the PIV technique were conducted in sand. The goal was to uncover the deformation mechanism of laterally loaded pile-soil systems under scour conditions. In addition, the size of the scour hole, the flexural rigidity of the piles, and the relative sand density of the soil were taken into account.

2 EXPERIMENTAL PROGRAMME

2.1 Test Soil and Preparation

Toyoura sand, a type of fine sand from Japan, is used in the model tests. The Specific gravity (G_s), maximum void ratio (e_{\max}), and minimum void ratio (e_{\min}) are 2.64, 0.98, and 0.60, respectively. In order to properly prepare soil samples, the soil's dry density (ρ_d), as determined by Eq. (1), must be controlled.

$$\rho_d = \frac{G_s \rho_w}{1 + e} \quad (1)$$

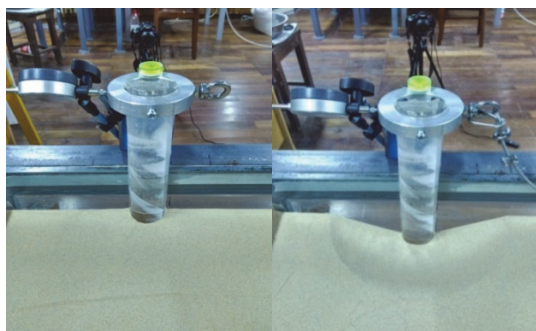
where G_s stands for the specific gravity of soil, e for the void ratio of soil, and ρ_w for water density. Once the predicted relative density (D_r), the maximum void ratio (e_{\max}), and minimum void ratio (e_{\min}) of the soil are known, the void ratio of soil (e) can be simply estimated by Eq. (2):

$$e = e_{\max} - D_r (e_{\max} - e_{\min}) \quad (2)$$

2.2 Experimental Setups

The front wall, back wall, and side wall of the testing chamber are separated from the pile axis by more than 6D, 3D, and 3D, respectively (where D is the diameter of the pile), in order to minimize the influence of borders. The testing chamber's side walls are composed of two plates of steel and two plates of tempered glass. A pulley that can be readily adjusted for height and horizontal direction to apply lateral loads at the pile head is mounted on one of the side walls of the steel plate.

The model pile is made of a solid plexiglass rod that is sliced along the symmetrical axis of the circular section. Model piles are divided into two categories based on their 2 cm and 5 cm diameters. The width of the testing chamber is a dozen times larger than the model pile diameter, so it is large enough to avoid boundary effects [15]. The model pile will be placed close to one side wall of the tempered glass panel during testing shown in Fig. 2, and a pull ring and an aluminum alloy ring are attached to the pile head for lateral loading.



(a) non-scour around the pile (b) a scour pit around the pile
Figure 2 Layout of the model pile in the testing chamber

A digital camera with automatic focusing (Canon, EOS400D) is used for all experiments. The camera's image pixels can reach 10 million. A corresponding camera bracket allows for height-based positioning adjustment of the camera.

2.3 Scour Hole

The three-dimensional (3D) scour hole is modelled following [8] as a circular cone with the top inverted and truncated. According to the specific dimensions of the scouring depth, scour width, and slope angle of the local scour hole, it needs to excavate the soil surrounding the pile.

2.4 Test Schedule

There are eight tests: tests T1 through T4 represent those that do not consider scour, while the remaining tests represent those that do consider a 3D scour hole surrounding the pile. In experiments, two different types of model piles are used: pile A has a diameter of 2 cm and a flexural rigidity (EI) of 12.2 N·m, pile B has a diameter of 5 cm and a flexural rigidity (EI) of 475.5 N·m. Two types of sandy soil are considered in tests for non-scour conditions: loose sand ($D_r = 35\%$) and medium-dense sand ($D_r = 60\%$), however only medium-dense sand is used in tests that take scouring into account. Overall length of the model piles is 48.5 cm, and the embedded portion is 30 cm.

Tests of TS1~TS4 were conducted in medium-density sand with two different scour pit dimensions: one with a scour depth of 2.5 cm and a scour width of 5 cm, and the other with a scour depth of 5 cm and a scour width of 10 cm. The test schedule is displayed in Tab.1.

Table 1 Test schedule

Test number	Model pile	Sand	Scour depth S_d / cm	Scour width S_w / cm	flexural rigidity EI / N·m ²
T1	A	loose	Non-scour		12.2
T2		medium			
T3	B	loose	Non-scour		475.5
T4		medium			
TS1	A	medium	2.5	5	12.2
TS2			5	10	
TS3	B	medium	2.5	5	475.5
TS4			5	10	

2.5 Test Procedure

The pulley will be adjusted to the transparent side wall through the horizontal sliding rod before loading. For all tests, lateral loads are applied 185 mm above the pre-scour ground surface. Fig. 3 depicts an experimental loading diagram under scouring conditions, and the following are the key testing procedures:

(1) The model pile is tightly attached to the transparent side wall, 15 cm above the testing chamber's bottom. A specific amount of dry sand is poured into the testing chamber with a thickness of every 5 cm in accordance with the anticipated sand relative density, compacted smoothly to the predetermined position layer by layer. The model pile is kept vertical with the aid of a levelling bubble and a levelling ruler until the sand filling is complete. Excavate

the soil carefully around the pile foundation in the light of the scour hole's specific depth, width, and slope angle.

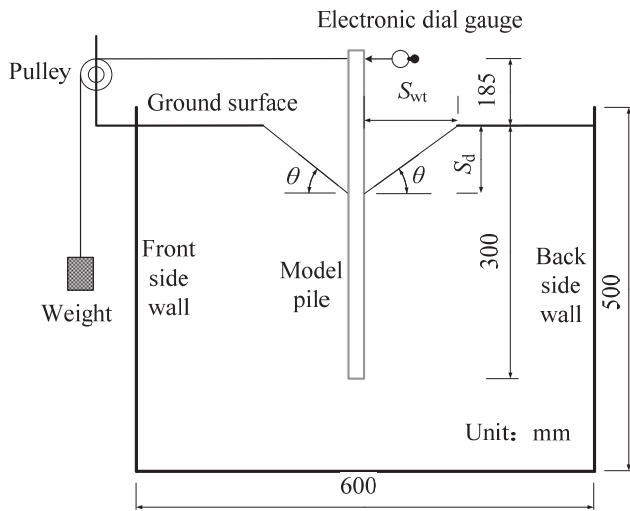


Figure 3 Schematic of test loading under scour condition

(2) Mount the digital dial gauge at the pile head. Place the camera 2.0 m away from the transparent side wall of the testing chamber, and keep it there throughout the duration of the test. Pay close attention to the lighting when taking test photos to ensure they are of the highest calibre.

(3) To determine the loading levels, a preloading test is used for each test. Each time a loading step is completed, the electronic dial gauge records the value and an experimental picture is taken when the model pile's lateral displacement stops increasing. Approximately ten successive loading steps are used to finish each experiment.

3 TEST RESULTS AND ANALYSIS

The photos obtained during each test are processed using the GeoPIV programme created by White and Take

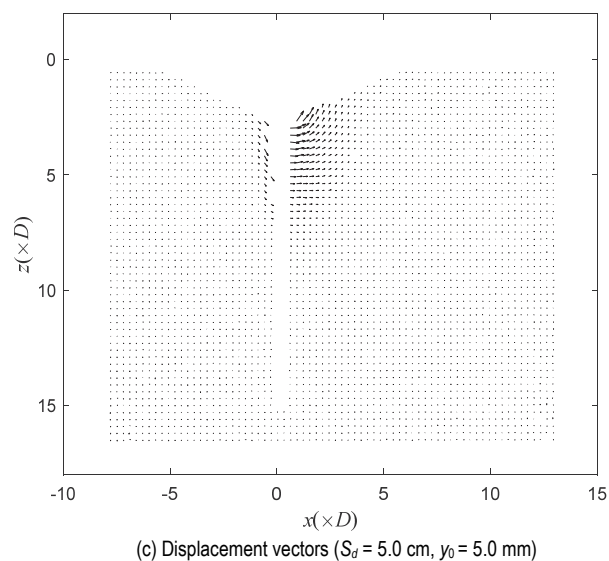
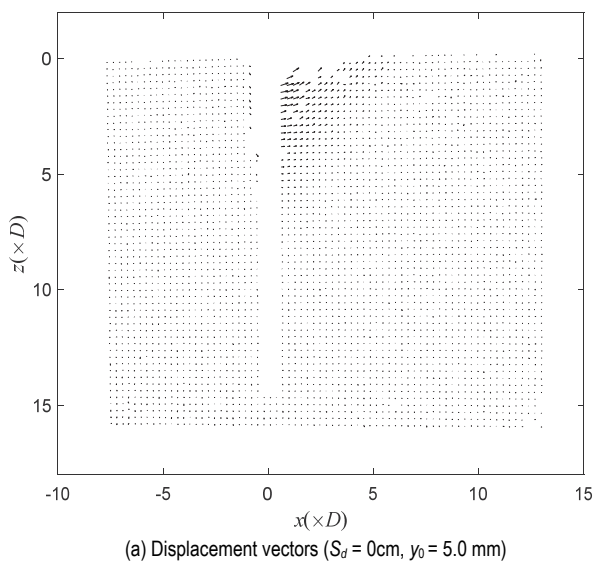
[9]. The side views of the soil displacement fields and soil strain fields at the pile side can be acquired through pre-processing, image analysis, and post-processing in the style of man-machine interaction.

When the lateral displacement (y_0) at the pile head is around 5 and 20 mm, respectively, the displacement vectors and strain contours of the soil surrounding the pile are presented below using the PIV technique. Pixel coordinate systems for all of the images have been transformed into Cartesian coordinate systems and normalised by pile diameter D . In Fig. 4 to Fig. 7, the pile axis is located at $x = 0D$. The values of the soil strain contours in Fig. 5 and Fig. 7 are shown as percentages.

3.1 Test Results of Pile A ($D = 2$ cm)

Fig. 4 depicts the soil displacement vectors around pile A in medium-density sand with pile deflections of roughly 5 and 20 mm. The soil displacement vectors in (a) and (b) are those under non-scour conditions, while those in (c) and (d) are those under scour conditions with scour depths (S_d) of 5.0 cm. Regardless of the presence of scour, it is evident that soil deformation occurs primarily in two zones, the passive zone in front of the pile and the active zone behind the pile.

The soil deformation in the passive zone diminishes along the radial and vertical direction. Active zone soil becomes loose due to pile movement and slides into the space behind the pile shaft. Furthermore, it can be shown that, in the absence of scour, soil deformation generally takes place in the shallow soil layer and hardly ever happens towards the pile end, exhibiting the deformation characteristics of a flexible pile (Fig. 4b). However, when a scour pit surrounds the model pile with a larger deflection shown in Fig. 4d, it can be observed that obvious soil deformation occurs at the pile end, making the model pile's lateral response appear to be that of a semi-rigid pile, whose soil-pile stiffness lies between that of rigid and flexible piles.



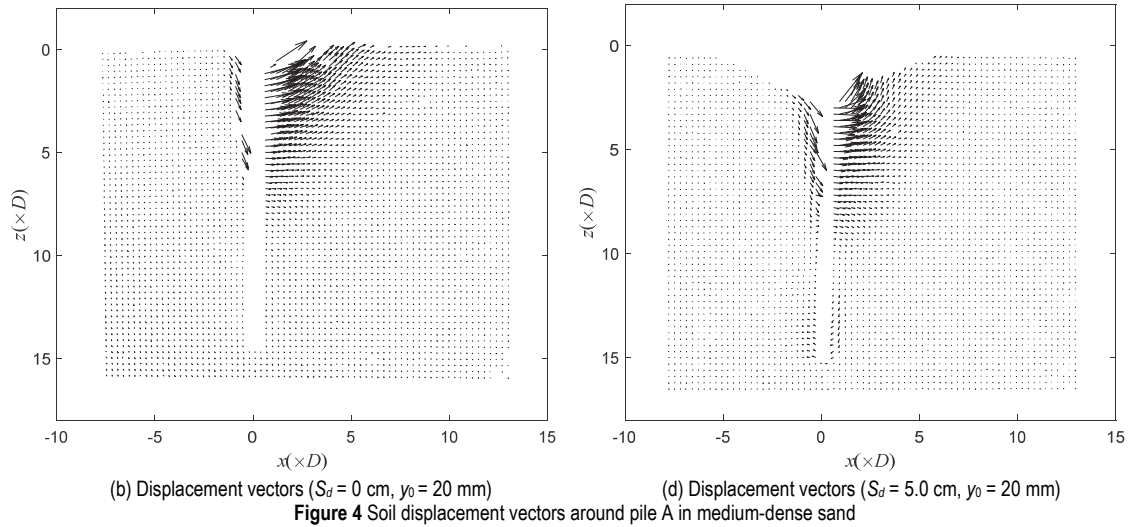
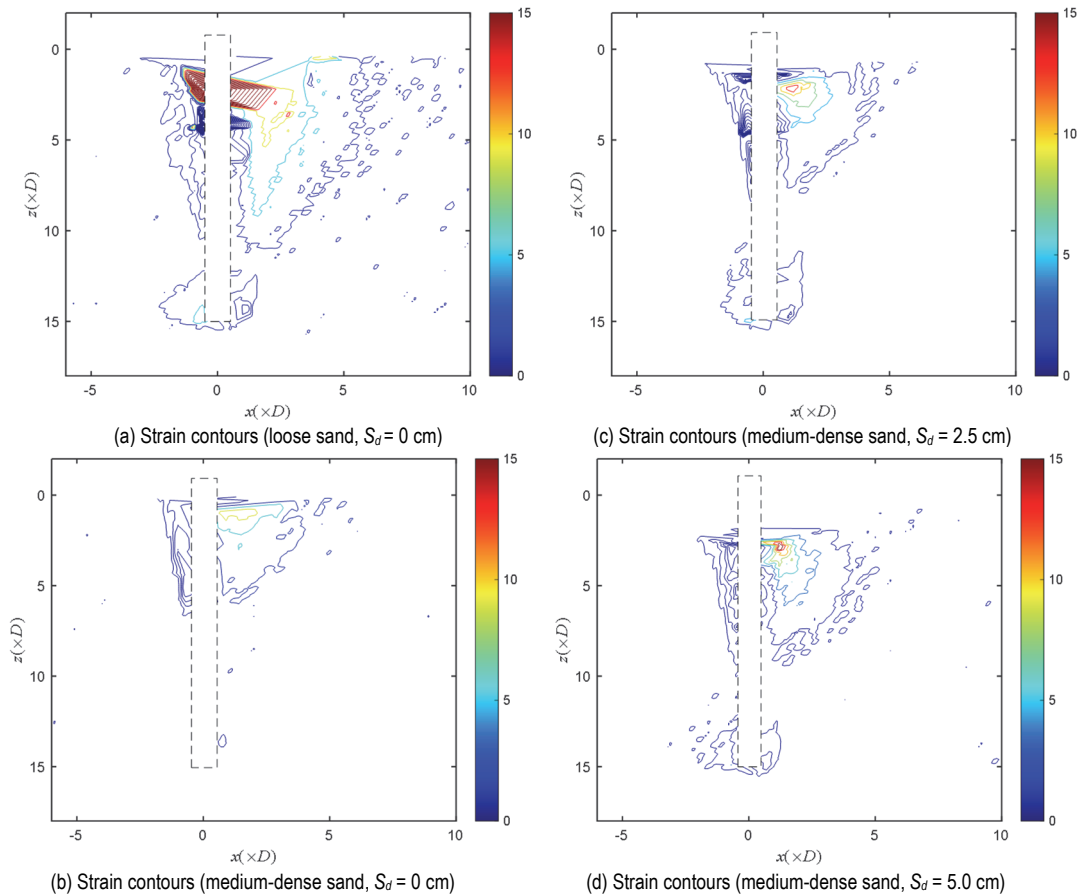


Fig. 5 shows contours of soil strain in the x direction (ϵ_{xx}) around model pile A with a pile deflection of about 20 mm, where (a) and (b) are soil strain contours in loose and medium-sand respectively both under non-scour conditions, (c) and (d) are soil strain contours around the model pile with a local scour pit of scour depths (S_d) of 2.5 cm and 5.0 cm both in medium-sand respectively. The model pile's lateral response resembles that of a semi-rigid pile in loose sand (Fig. 5a), where it can be seen that the soil deforms more significantly near the pile end. In contrast, there is no visible deformation at the pile end in

medium-dense sand, as shown in Fig. 4b, which depicts the lateral response of a flexible pile. Although the soil in Fig. 5c and Fig. 5d is medium-density sand, soil strain contours show that the model pile behaves like a semi-rigid pile and appears to be in loose sand without scour. This behaviour may be due to the soil effective stress dropping brought on the soil erosion around the pile. Under scour conditions, the characteristics of the distribution of soil strain and the development laws in the passive zone and active zone are essentially the same as under non-scour conditions.



3.2 Test Results of Pile B ($D = 5\text{ cm}$)

Experimental results for model pile B with pile deflections of approximately 5 and 20 mm in medium-dense sand are displayed in Fig. 6. In this figure, (a) and (b) represent soil displacement vectors under non-scour conditions, and (c) and (d) represent soil displacement vectors under scour conditions with a scour depth (S_d) of 5.0 cm. Soil displacement in the passive zone develops along the radial and deeper soil layers, similar to

how model pile A deforms, whereas in the active zone, the soil slides down behind the pile body. In contrast to the deformation characteristics of pile A under non-scour conditions, in which pile A behaves like a semi-rigid pile in loose sand and a flexible one in medium-dense, tests of pile B under non-scour conditions present the rigid short piles features that an obvious rotation centre is at a distance of approximately $0.75 L$ (L =pile embedded length) far from the ground surface.

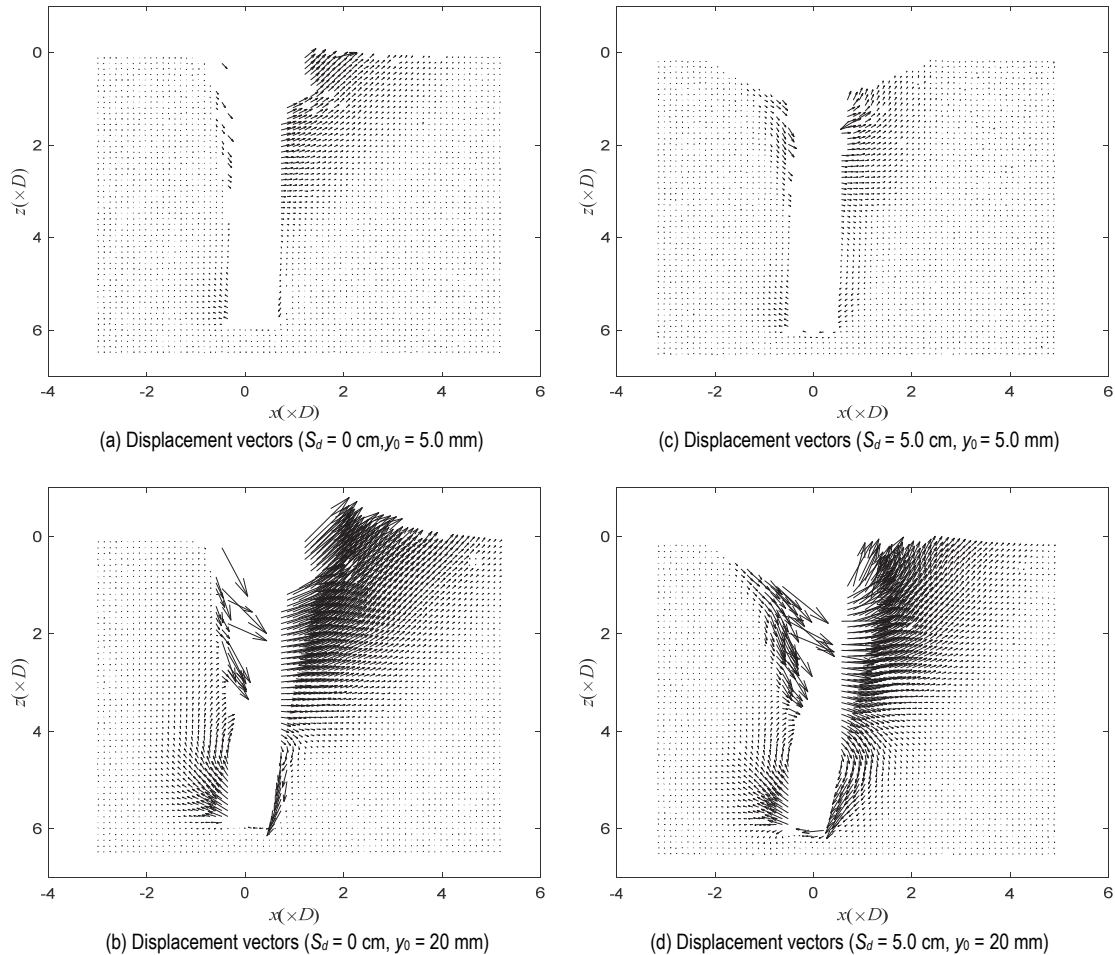
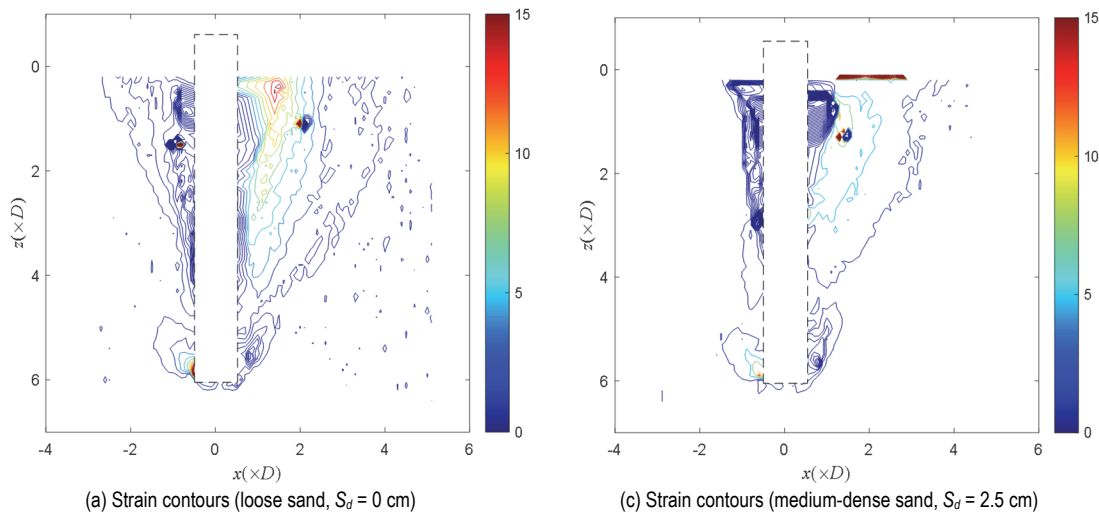
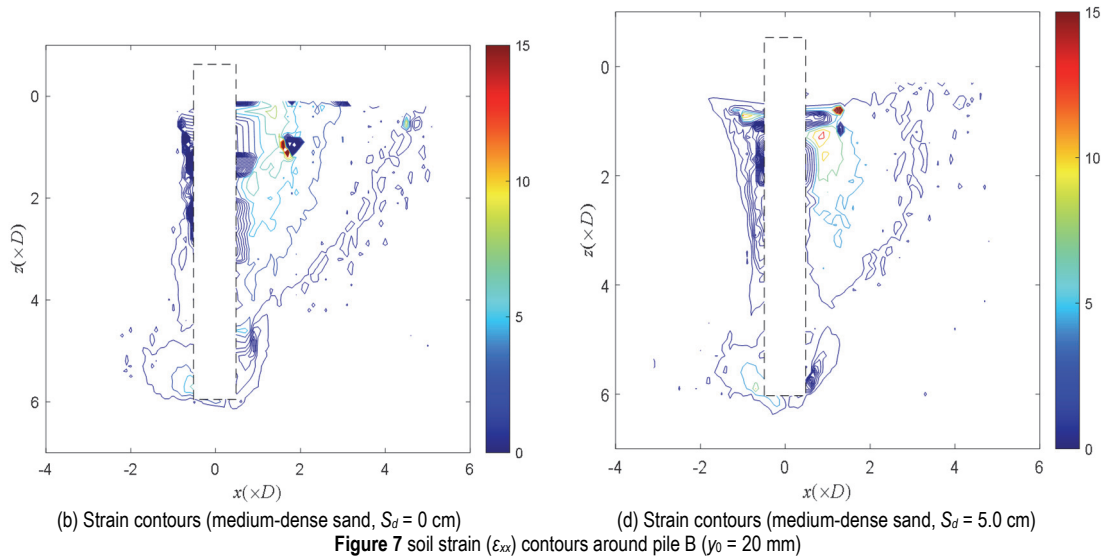


Figure 6 Soil displacement vector around pile B in medium-dense sand





Soil strain (ϵ_{xx}) contours for tests of model pile B are displayed in Fig. 7, where (a) and (b) represent strain contours in loose sand and in medium-density sand respectively, and both under non-scour conditions, (c) and (d) represent strain contours with a local scour pit of scour depths (S_d) of 2.5 cm and 5.0 cm, respectively, in medium-density sand. Although there is a greater displacement at the pile end in deeper soil layers, whether in tests with or without scour, it is clear that the basic characteristics of soil strain distribution and development in the passive zone and active zone around the pile are essentially consistent with those of pile A in shallow soil layers.

Soil erosion around the pile foundations will surely cause the pile to become more stiff by decreasing the effective stress of the soil and the embedded pile length-diameter ratio. It shows that the soil strains in the passive zone are not constant and gradually change in the radial and vertical direction in all of the tests when the lateral load on the pile top increases.

4 DISCUSSION

The experimental program provided new insights into the deformation behavior of laterally loaded piles subjected to different scour conditions. In all cases, the soil deformation was primarily concentrated in two distinct zones: the passive zone in front of the pile and the active zone behind the pile. This observation is consistent with the basic soil-pile interaction mechanism under lateral loading. For pile A, with a smaller diameter and lower flexural rigidity, the lateral response exhibited flexible characteristics (see Fig. 8a) in medium-dense sand and semi-rigid behavior (see Fig. 8b) in loose sand. Pile B, with a larger diameter and higher flexural rigidity, consistently behaved as a rigid pile under both loose and medium-dense sand conditions. Under scour conditions, the effective stress in the surrounding soil decreased, causing pile A in medium-dense sand to behave similarly to a semi-rigid pile in loose sand without scour. This highlights the critical influence of scour on reducing pile-soil stiffness and altering the load transfer mechanism along the pile shaft.

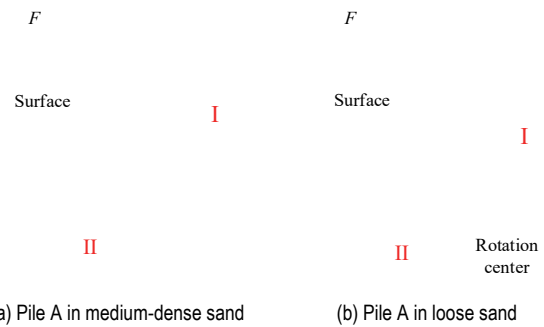


Figure 8 Schematic of pile behavior in sand with different relative densities

The deformation patterns identified in this study can be compared with previous research that applied image-based techniques such as PIV and DIC. Hajjalilue-Bonab et al. [12] proposed a three-dimensional strain wedge model based on PIV analysis, showing soil deformation extending in the form of a conical wedge. Suleiman et al. [13] used DIC to observe soil movement up to 6.3 pile diameters from the pile center, which agrees with the large deformation zones captured in our experiments. Yuan et al. [14] further developed a 3D monitoring system in transparent soil, confirming the complex deformation fields around laterally loaded piles. The findings in this study align with the above studies in demonstrating significant soil displacement in both radial and vertical directions, while also extending the knowledge by explicitly addressing the additional effects of scour holes. In particular, the transition from flexible to semi-rigid behavior observed in pile A under scour conditions has not been widely reported in previous literature, and therefore provides a new perspective on scour-pile interaction.

The results have important implications for the design of pile foundations in bridges, ports, and offshore wind structures. In engineering practice, scour around pile foundations is often treated conservatively by reducing the embedment depth. However, our findings suggest that this approach may oversimplify the actual soil-pile interaction mechanisms. Scour not only decreases effective embedment but also alters the soil stiffness around the pile, leading to changes in the pile response mode (e.g., from flexible to semi-rigid). This behavior can significantly

influence the lateral displacement and bending moments along the pile shaft. For rigid piles such as pile B, scour further accentuated the concentration of soil deformation near the pile tip, which may result in unexpected failure modes. Therefore, design guidelines should consider not only the reduction in embedment depth but also the transformation of soil-pile stiffness due to scour. This would lead to more accurate predictions of pile performance and improved safety margins in geotechnical design.

Despite the valuable insights provided, some limitations must be acknowledged. First, only two pile diameters were tested, which may not fully capture the scale effects that influence pile-soil interaction under scour conditions. Second, the soil used in the experiments was Toyoura sand with two relative densities, whereas natural field conditions may involve a wider range of soil types, including cohesive soils, layered deposits, or mixed seabed conditions. Third, the study considered only static lateral loading, while cyclic or dynamic loading from waves, currents, and earthquakes is often critical in offshore environments. Finally, the pile models were conventional solid plexiglass rods, which lack structural innovations in pile-making methods. Addressing these limitations in future research would strengthen the generalizability and engineering applicability of the findings.

The lateral loads acting on piles are primarily induced by wind and wave actions, while vertical loads (V) mainly arise from the self-weight of the turbine. With the emergence of larger and heavier energy converters in recent years, the impact of vertical loading on the overall stability performance of pile has become increasingly prominent. The influence of vertical loading has not yet been addressed in this study. Vertical loading gives rise to the $P-A$ effect, thereby exerting a significant impact on the lateral displacement of the pile foundation. This will be the focus of our future work.

Piles with headed beams or alternative structural configurations may enhance the lateral resistance of pile foundations under scour conditions. Comparative model tests between conventional piles and innovative piles will allow for a direct evaluation of their relative performance, and will provide evidence-based recommendations for design improvement. Additionally, numerical modeling tools such as finite element analysis and advanced $p-y$ curve formulations can be combined with experimental results to extend the analysis to a wider range of boundary conditions. Cyclic and dynamic load tests should also be conducted in future work to reflect more realistic loading scenarios in offshore and hydraulic structures.

5 CONCLUSION

A series of model tests of laterally loaded piles are conducted using the PIV technique, with consideration given to the relative density of the sand, the flexural rigidity of the pile body, and the 3D dimensions of the scour pit. For every loading step in each test, experimental images are recorded, and then soil displacement vectors and contours of soil strain (ϵ_{xx}) are obtained using the PIV technique, and soil strain distribution and development characteristics are analysed. The following conclusions can be drawn.

(1) All of the experimental findings suggest that as the lateral load supplied to the pile head increases, soil displacements and soil strains in the passive zone in front of the model pile gradually develop in radial and vertical directions. Due to the movement of the pile body, sand soil in the active zone behind the pile becomes loosened and slips into a gap behind the model pile.

(2) For tests without scouring, pile A acts as a semi-rigid pile in loose sand, but as a flexible pile in medium-density sand, while pile B acts as a rigid pile in both loose sand and medium-density sand, and an obvious rotation center occurs at the lower part of the pile shaft when a larger lateral deflection is on the pile head.

(3) Although the soil in the experiments for pile A with scouring is medium-density sand, the soil displacement and strain characteristics at the pile side resemble those in loose sand without scouring, and the model pile exhibits semi-rigid characteristics. The primary cause is the local scour, which reduces the effective stress of the top soil layer and results in a smaller aspect ratio of the pile and a different form of lateral response of piles. When soil erosion develops near pile B, the pile tends to act more rigidly.

(4) The results indicate that design approaches considering only the reduction of embedment depth may underestimate the true impact of scour. The observed transformation of pile behavior (flexible \rightarrow semi-rigid \rightarrow rigid) suggests that design guidelines should explicitly account for stiffness changes induced by scour. This insight is particularly relevant for offshore wind turbine foundations, bridge piers, and port structures.

The current experiments were limited to two pile diameters, two sand densities, and scour depths of 2.5 and 5 cm. Although these conditions provide meaningful insights, they do not cover the full range of practical scenarios. Future work will expand the test matrix to include larger scour depths and broader pile geometries, as well as cyclic and dynamic loadings. Furthermore, innovative pile configurations such as headed-beam piles will be investigated to evaluate potential design improvements.

Overall, this study highlights the importance of scour as a factor that fundamentally alters soil-pile interaction, not only by reducing embedment but also by modifying deformation patterns and pile stiffness regimes. These findings provide both a basis for further research and practical implications for the safe design of pile foundations in scoured environments.

Acknowledgements

The authors acknowledge Anhui Provincial Natural Science Foundation (Grant No.1908085QE214), the PhD Foundation of Anhui University of Science and Technology (Grant No.12367) for the financial support and the Natural Science Research Project of Anhui Educational Committee (Grant No. 2024AH050353).

6 REFERENCES

- [1] Sumer, B. M., Fredsøe, J., & Christiansen, N. (1992). Scour around vertical pile in waves. *Journal of Waterway, Port, Coastal, and Ocean Engineering*, 118(1), 15-31.

- [https://doi.org/10.1061/\(ASCE\)0733-950X\(1992\)118:1\(15\)](https://doi.org/10.1061/(ASCE)0733-950X(1992)118:1(15))
- [2] Zhao, M., Cheng, L., & Zang, Z. (2010). Experimental and numerical investigation of local scour around a submerged vertical circular cylinder in steady currents. *Coastal Engineering*, 57(8), 709-721. <https://doi.org/10.1016/j.coastaleng.2010.03.002>
- [3] Pandey, M., Zakwan, M., Khan, M. A., & Swati, B. (2020). Development of scour around a circular pier and its modelling using genetic algorithm. *Water Supply*, 20(8), 3358-3367. <https://doi.org/10.2166/ws.2020.244>
- [4] Aly, A. M. & Dougherty, E. (2021). Bridge pier geometry effects on local scour potential: A comparative study. *Ocean Engineering*, 234, 109326. <https://doi.org/10.1016/j.oceaneng.2021.109326>
- [5] Yang, X., Zhang, C., Huang, M., & Yuan, J. (2018). Lateral loading of a pile using strain wedge model and its application under scouring. *Marine Georesources & Geotechnology*, 36(3), 340-350. <https://doi.org/10.1080/1064119X.2017.1317889>
- [6] Liang, F., Zhang, H., & Chen, S. (2018). Effect of vertical load on the lateral response of offshore piles considering scour-hole geometry and stress history in marine clay. *Ocean Engineering*, 158, 64-77. <https://doi.org/10.1016/j.oceaneng.2018.03.070>
- [7] Yu, F., Zhang, C., Huang, M., Yang, X., & Yao, Z. (2022). Scouring effects on lateral cyclic responses of piles in sand. *European Journal of Environmental and Civil Engineering*, 27(5), 1941-1956. <https://doi.org/10.1080/19648189.2022.2107082>
- [8] Qi, W. G., Gao, F. P., Randolph, M. F., & Lehane, B. M. (2016). Scour effects on p-y curves for shallowly embedded piles in sand. *Geotechnique*, 66(8), 648-660. <https://doi.org/10.1680/jgeot.15.P.157>
- [9] White, D. J., Take, W. A., & Bolton, M. D. (2003). Soil deformation measurement using particle image velocimetry (PIV) and photogrammetry. *Geotechnique*, 53(7), 619-631. <https://doi.org/10.1680/geot.2003.53.7.619>
- [10] Liu, J., Yuan, B., Mai, V. T., & Dimaano, R. (2011). Optical measurement of sand deformation around a laterally loaded pile. *Journal of Testing and Evaluation*, 39(5), 754-759. <https://doi.org/10.1520/JTE103313>
- [11] Yuan, B., Sun, M., Xiong, L., Luo, Q., Pradhan, S. P., & Li, H. (2020). Investigation of 3D deformation of transparent soil around a laterally loaded pile based on a hydraulic gradient model test. *Journal of Building Engineering*, 28, 101024. <https://doi.org/10.1016/j.job.2019.101024>
- [12] Hajjalilue-Bonab, M., Sojoudi, Y., & Puppala, A. J. (2013). Study of strain wedge parameters for laterally loaded piles. *International Journal of Geomechanics*, 13(2), 143-152. [https://doi.org/10.1061/\(ASCE\)GM.1943-5622.0000186](https://doi.org/10.1061/(ASCE)GM.1943-5622.0000186)
- [13] Suleiman, M. T., Ni, L., Raich, A., Helm, J., & Ghazanfari, E. (2015). Measured soil-structure interaction for concrete piles subjected to lateral loading. *Canadian Geotechnical Journal*, 52(8), 1168-1179. <https://doi.org/10.1139/cgj-2014-0197>
- [14] Yuan, B., Sun, M., Wang, Y., Zhai, L., Luo, Q., & Zhang, X. (2019). Full 3D displacement measuring system for 3D displacement field of soil around a laterally loaded pile in transparent soil. *International Journal of Geomechanics*, 19(5), 04019028. [https://doi.org/10.1061/\(ASCE\)GM.1943-5622.0001409](https://doi.org/10.1061/(ASCE)GM.1943-5622.0001409)
- [15] Albiker, J., Achmus, M., Frick, D., & Flindt, F. (2017). 1g model tests on the displacement accumulation of large-diameter piles under cyclic lateral loading. *Geotechnical Testing Journal*, 40(2), 173-184. <https://doi.org/10.1520/GTJ20160102>

Contact information:

Xiaofeng YANG, PhD, Lecturer
School of Civil Engineering and Architecture,
Anhui University of Science and Technology,
Huainan, Anhui 232001, China
E-mail: xiaofengsile@163.com

Zhenwei HE, Student
School of Civil Engineering and Architecture,
Anhui University of Science and Technology,
Huainan, Anhui 232001, China
E-mail: hzhenwei_96@163.com

Feng YU, PhD, Lecturer
(Corresponding author)
School of Civil Engineering and Architecture,
Anhui University of Science and Technology,
Huainan, Anhui 232001, China
E-mail: 2021061@aust.edu.cn